Analytica Chimica Acta 744 (2012) 33–38

Contents lists available at SciVerse ScienceDirect

Analytica Chimica Acta

journal homepage: www.elsevier.com/locate/aca

Visible light induced photoelectrochemical biosensing based on oxygen-sensitive quantum dots

Wenjing Wang, Lei Bao, Jianping Lei*, Wenwen Tu, Huangxian Ju*

State Key Laboratory of Analytical Chemistry for Life Science, Department of Chemistry, Nanjing University, Nanjing 210093, PR China

HIGHLIGHTS

- The near-infrared QDs are synthesized in an aqueous solution.
- QDs-based biosensor exhibits visible-light induced cathodic photocurrent.
- The oxygen dependency of the photocurrent is verified.
- A photoelectrochemical strategy is established by coupling with enzymatic reaction.
- Photoelectrochemical sensor shows high upper detection limit, acceptable stability and accuracy.

GRAPHICAL ABSTRACT

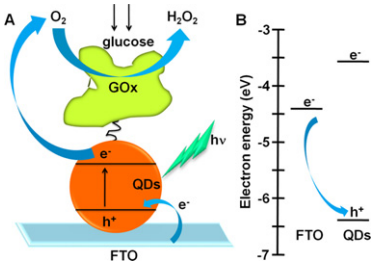

ARTICLE INFO

Article history:
Received 12 May 2012
Received in revised form 12 July 2012
Accepted 17 July 2012
Available online 22 July 2012

Keywords:
Photoelectrochemistry
Near-infrared quantum dots
Biosensing
Enzyme
Glucose

ABSTRACT

A visible light induced photoelectrochemical biosensing platform based on oxygen-sensitive near-infrared quantum dots (NIR QDs) was developed for detection of glucose. The NIR QDs were synthesized in an aqueous solution, and characterized with scanning electron microscopy and X-ray photoelectron spectroscopy. The as-prepared NIR QDs were employed to construct oxygen-sensitive photoelectrochemical biosensor on a fluorine-doped tin oxide (FTO) electrode. The oxygen dependency of the photocurrent was investigated at as-prepared electrode, which demonstrated the signal of photocurrent is suppressed with the decreasing of oxygen. Coupling with the consumption of oxygen during enzymatic reaction, a photoelectrochemical strategy was proposed for the detection of substrate. Using glucose oxidase (GOx) as a model enzyme, that is, GOx was covalently attached to the surface of CdTe QDs, the resulting biosensor showed the sensitive response to glucose. Under the irradiation of visible light of a wavelength at 505 nm, the proposed photoelectrochemical method could detect glucose ranging from 0.1 mM to 11 mM with a detection limit of 0.04 mM. The photoelectrochemical biosensor showed a good performance with high upper detection limit, acceptable stability and accuracy, providing an alternative method for monitoring biomolecules and extending the application of near-infrared QDs.

1. Introduction

Photoelectrochemical biosensing is a newly emerged analytical technique, which uses light to induce electron transfer between photoelectrochemical-active species and electrode for generating the detectable photocurrent signal [1–7]. Since the complete separation of excitation source (light) and detection signal (current), the undesired background signal is greatly reduced. Thus, photoelectrochemical technique possesses potentially higher sensitivity than the conventional electrochemical and optical methods [8,9]. A series of photoelectrochemical platforms have been designed by using biotinylated tris(bipyridyl) ruthenium(II) complex [1], TiO_2 nanotubes [3], CdSe [4], porphyrin-functionalized ZnO nanoparticles [7], and rhodamine–ployaniline [10]. Although the above

* Corresponding authors. Tel.: +86 25 83593593; fax: +86 25 83593593.
E-mail addresses: jpl@nju.edu.cn (J. Lei), hxju@nju.edu.cn (H. Ju).

0003-2670/$ – see front matter © 2012 Elsevier B.V. All rights reserved.
http://dx.doi.org/10.1016/j.aca.2012.07.025

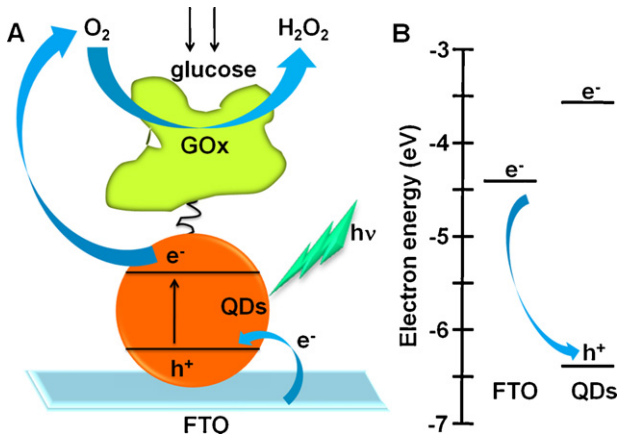

Scheme 1. Schematic illustration of the photoelectrochemical strategy for detection of glucose at GOx/CdTe/FTO electrode.

photoelectrochemical platforms exhibit good performance for the detection of biomolecules, their applications are limited in biological systems due to the ultraviolet light irradiation. Thus it is significant to explore the new photosensitive materials in order to apply the photoelectrochemical platforms in bioanalysis.

Quantum dots (QDs) are the excellent candidates in the development of optical and photoelectrochemical biosensing since they have the broad excitation spectrum, good photostability, and tunable emission spectrum [11–16]. For example, a photoelectrochemical sensor based on CdS–polyamidoamine nanocomposite film was developed for cell capturing and detection under the light irradiation with 430 nm wavelength [17]. However, since 99% of the energy output from the sun is in the visible range, it is desirable for photosensitizers to absorb visible light in the development of photoelectrochemical devices [18]. Moreover, for medical applications, the light in the near-infrared range is efficient as it penetrates more deeply into tissues. Therefore, the near-infrared quantum dots (NIR QDs) with emission wavelengths between 650 and 900 nm have attracted considerable attention for multicolor labeling in biological systems [19–21]. The NIR QDs-based photoelectrochemical platform could enhance the absorption in the visible range and increase the lifetime of charge carriers [22]. In this work, a NIR QDs-based photoelectrochemical platform was constructed for the detection of glucose under visible light irradiation.

Glucose as the substrate of glucose oxidase (GOx) is oxidized to gluconolactone in the presence of O_2 via enzymatic reaction, while O_2 was reduced to H_2O_2. Based on oxygen consumption, the photocurrent is suppressed since O_2 is employed as electron acceptor during the photoelectrochemical process [23]. Here, integrating the specificity of GOx with the advantages of photoelectrochemical biosensing, a fast and sensitive photoelectrochemical measurement of glucose was achieved by using NIR QDs at a fluorine-doped tin oxide (FTO) electrode (Scheme 1). The NIR CdTe QDs were prepared in aqueous solution with 3-mercaptopropionic acid as stabilizer, and then doped on FTO as working electrode. In the presence of dissolved oxygen as electron acceptor, the as-prepared biosensor exhibited significant visible-light induced cathodic photocurrent under 505 nm light excitation. Upon addition of glucose, due to the oxygen-consumption via enzymatic reactions, the photocurrent dramatically decreased with the increasing of glucose, resulting in a photoelectrochemical strategy for the detection of glucose. This facile photoelectrochemical biosensor showed high upper detection limit and wide linear range. This visible light photoelectrochemical sensing platform would provide a generic approach to analyze numerous substances in bioanalysis.

2. Experimental

2.1. Chemicals and materials

Glucose oxidase (GOx, G7141-50 KU), 3-mercaptopropionic acid (MPA, ≥99%), 1-ethyl-3-(3-dimethylaminopropyl) carbodiimide (EDC), *N*-hydroxysuccinimide (NHS), tris(hydroxymethyl)-aminomethane hydrochloride and tris(hydroxymethyl)-aminomethane (Tris, reagent grade) were purchased from Sigma Chemical Co. (MO, USA). Cadmium chloride ($CdCl_2{\cdot}2.5H_2O$) was purchased from Alfa Aesar China Ltd. (China). Tellurium rod (4 mm in diameter) was purchased from Leshan Kayada Photoelectricity Co. (China). D-(+)-Glucose was bought from Sinopharm Chemical Reagent Co., Ltd. (China). Glucose injection was purchased from local clinique (Jiangxi Kelun Pharmaceutical Co., Ltd. and Shandong Hualu Pharmaceutical Co., Ltd.). FTO membrane covered glass as the electrode material was purchased from Beijing Midwest Group Technology Co., Ltd. (China). All other chemicals were of analytical grade and without further purification.

GOx was dissolved in phosphate-buffered saline solution (PBS, 10 mM, pH 7.4) to obtain a solution (2.0 mg mL^{-1}) that was stored at 4 °C. Glucose stock solution was mutarotated overnight at room temperature prior to use. Tris–HCl (0.1 mol L^{-1}) was employed as supporting electrolyte during the photoelectrochemical procedure. The pH of Tris–HCl was 7.0 unless indicated otherwise. Aqueous solutions in the entire work were prepared with ultrapure water from a Millipore water purification system (≥18 MΩ, Milli-Q, Millipore).

2.2. Instrumentation

Scanning electron microscopic (SEM) images were obtained using a Hitachi S-4800 scanning electron microscope (Japan). The transmission electron microscopic (TEM) images were gained on a JEM-2100 TEM (JEOL, Japan). X-ray photoelectron spectra (XPS) were obtained using an ESCALAB 250 spectrometer (Thermo-VG Scientific, USA) with ultra-high vacuum generators. Ultraviolet-visible absorption spectra were recorded using a UV-3600 spectrometer (Shimadzu, Japan). The photoluminescence (PL) spectrum was recorded with RF-5301 PC fluorometer (Shimadzu, Japan). Fourier transform infrared (FT-IR) spectra were recorded on a Nicolet 400 FT-IR spectrometer (Madison, WI, USA). Photoelectrochemical detection was performed on Controlled Intensity Modulated Photo Spectrometer (Zahner Zennium, German) with a LW619 LED light (wavelength at 505 nm) as the accessory light source. All experiments were carried out at room temperature using a conventional three-electrode system with a modified FTO electrode as working, a platinum wire as auxiliary, and a saturated calomel electrode (SCE) as reference electrodes.

2.3. Synthesis of MPA–CdTe QDs

NIR CdTe QDs were prepared following the method reported method before [24,25]. Briefly, the Cd precursors were prepared by mixing the solution of $CdCl_2$ and stabilizer (MPA) solution, and then adjusted to pH 8.5 with 0.5 M NaOH. This solution was placed in a three-necked flask, fitted and deaerated with N_2 bubbled for 30 min. Under vigorous stirring, the prepared oxygen-free NaHTe solution was injected. The typical molar ratio of Cd:Te:MPA was 2:1:4.8 in our experiments. The resulting mixture solution was heated and refluxed for some time to obtain the QDs. The as-prepared QD solution was precipitated with the equivalent volume of acetone and collected by centrifugation. The colloidal precipitate

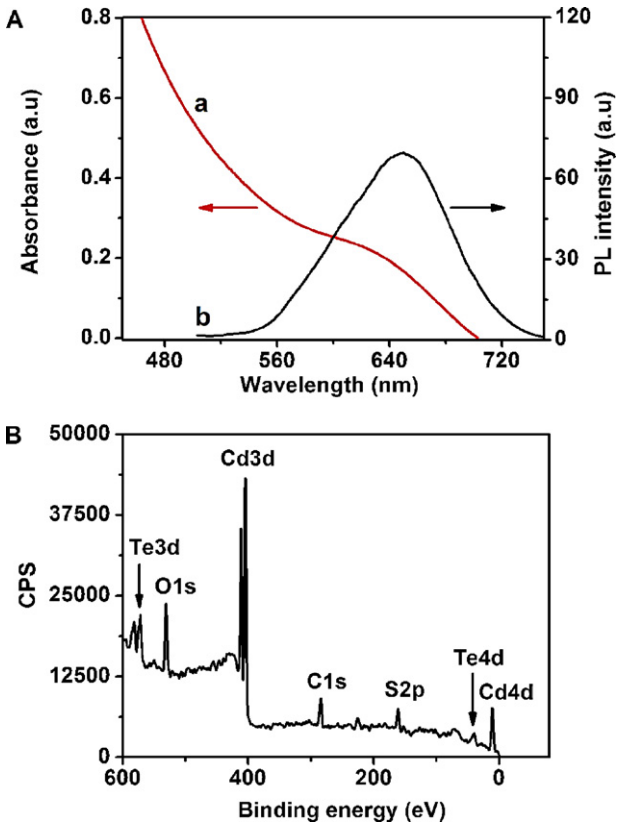

Fig. 1. (A) UV–vis absorption and fluorescence spectra of CdTe QDs, (B) XPS spectrum of CdTe QDs.

was redissolved in ultrapure water of one-tenth of the original volume and used as photosensitizer in subsequent experiments.

2.4. Modification of the electrode

After the FTO electrode had been cleaned with NaOH (0.5 mol L^{-1}) and H_2O_2 (30%), washed with acetone and twice-ultrapure water, and dried at room temperature, 10 μL of the QDs stock solution was coated onto a piece of FTO slice with a fixed area of 0.20 cm^2 and dried at room temperature to obtain an CdTe/FTO electrode. The resulting CdTe/FTO electrode was activated by casting 10 μL PBS containing 0.50 mg mL^{-1} of EDC and 0.25 mg mL^{-1} NHS for an hour. Then the activated electrode was thoroughly rinsed with water. Following this step, 10 μL of GOx solution was casted onto the CdTe/FTO electrode surface for the conjugation of the primary amine groups of GOx to the carboxyl groups of QDs. After incubated at room temperature for another 2 h, the GOx/CdTe/FTO electrode was obtained and stored at 4 °C overnight.

3. Results and discussion

3.1. Characterization of MPA–CdTe QDs

Fig. 1A shows the absorption and PL spectra of the as-prepared MPA–CdTe QDs. The resulting QDs show an absorption shoulder around 627 nm (Fig. 1A, curve a). According to the Peng's empirical equation [26], the diameter of QDs is estimated to be 3.95 nm, which could be attributed to the steric hindrance and electrostatic repulsion caused by the MPA. The TEM image of QDs shows that the distribution of diameter of CdTe QDs is from 3.84 nm to 5.20 nm (Fig. 2A), which is in good agreement with the result from the absorption spectrum. On the other hand, the PL spectrum of the as-prepared QDs showed a strong emission peak at 650 nm (Fig. 1A, curve b). The wavelength of the emission peak is consistent with the inflection point of UV–vis absorption, indicating the band gap emission of the core. Since the peak wavelength (at 650 nm) places in the NIR spectral region (650–900 nm), the excitation of visible light (505 nm) is enough to generate a cathodic photocurrent, which could reduce mischief to the samples, leading to a potential application in photoelectrochemical biosensing.

XPS was used to characterize the composition of as-prepared CdTe QDs. As shown in Fig. 1B, the XPS survey exhibited the two strong peaks at the binding energies of 404.5 and 572.4 eV, corresponding to the Cd3d and Te3d levels of the CdTe QDs, respectively. Carbon (284.4 eV of C1s), oxygen (531.8 eV of O1s), and sulfur (161.1 eV of S2p) from the organic ligands were also observed in the XPS spectrum. Moreover, the Cd/Te atoms ratios obtained from XPS data is 5.2, which indicates that most Cd atoms at the QD surface are stabilized by thiol ligands instead of Te atoms. This core–shell like structure obviously prevented the oxidation of Te, leading to a stable structure of the QDs [27].

3.2. Characterization of CdTe/FTO electrode

The CdTe/FTO electrode was prepared by casting the QDs stock solution onto the FTO electrode at room temperature. As shown in Fig. 2B, the SEM morphology of the QDs film exhibited a uniform layer with the aggregate size less than 30 nm. This size range was much smaller than 860 nm for unmodified CdTe QDs [28], probably due to the electrostatic repulsion among these negatively charged caps (MPA^{2-}) around CdTe cores. The decline in aggregation and the homogeneous surface structure are favorable for improving the photoelectrochemical efficiency.

After GOx was covalently attached to the surface of CdTe QDs via amide reaction, the vibration of amide I and amide II of GOx could be observed at 1653 and 1543 cm^{-1} (Fig. 2D, curve b), indicating the effective immobilization of GOx on the surface of CdTe QDs. The mushy configuration reveals that GOx has been well conjugated on the CdTe QDs (Fig. 2C). Therefore, the covalent coupling of GOx onto carboxyl group-coated CdTe QDs, using EDC-NHS as coupling reagents, is feasible, which provided a good stability of the photoelectrochemical biosensor.

3.3. Investigation of O_2 dependency of the photocurrent

In order to confirm the oxygen-sensitivity of this biosensor, the dependency should be investigated in the detection system. As shown in Fig. 3A, curve a, the photocurrent density of CdTe/FTO electrode was about 850 nA cm^{-2} in air-saturated buffer under the light irradiation with wavelength of 505 nm. When irradiated by suitable light, the direction of electron transfer was controlled by the energy level structure and the electric potential [29,30]. The mechanism of photocurrent should be explained as follows: Under the irradiation, the CdTe QDs were excited by visible light to generate e^-–h^+ separation between valence band (VB) and conduction band (CB). At the negatively applying bias, electrons from the CB of the QDs can reduce dissolved oxygen in the buffer, while the hole generated in VB of the QDs can be filled through electron transfer from the electrode. Thus a cathodic photocurrent will be generated under irradiation, leading to a photoelectrochemical biosensing (Scheme 1).

When nitrogen was purged into the buffer continuously, the oxygen content in solution is partially exchanged. After 20 min (curve b), an obvious decrease of the photocurrent intensity was observed, which is 12% than that of air-saturation solution. After adding the same concentration of 320 μM H_2O_2 as saturated

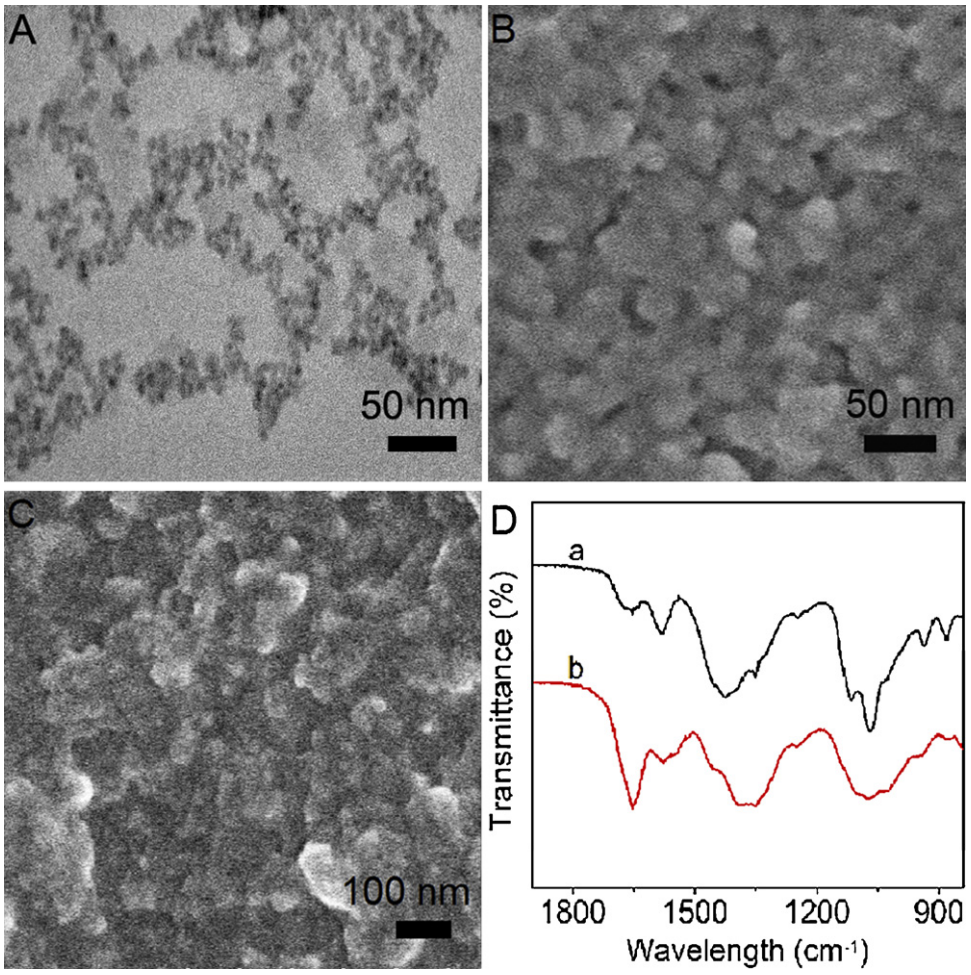

Fig. 2. (A) TEM image of CdTe QDs, SEM images of (B) CdTe QDs and (C) GOx/CdTe QDs on FTO electrode, (D) FT-IR spectra of CdTe QDs (a) and GOx/CdTe QDs (b).

dissolved O_2 into pH 7 Tris–HCl solution [31], the photocurrent only shows 23% than that of the initial current (curve c). These results suggest that oxygen as electron acceptor can be reduced by the generated electron during the irradiation of the QDs, and is more efficient than H_2O_2, thus, the cathodic photocurrent of QDs/FTO electrode with the dependence of dissolved O_2 could be desirable to construct an enzyme-based photoelectrochemical biosensing platform.

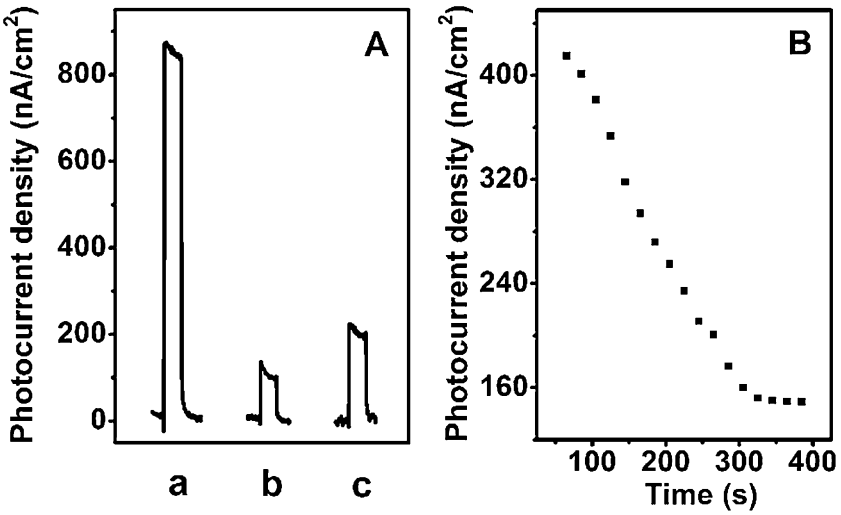

Fig. 3. (A) Photocurrent responses of CdTe/FTO electrode in air-saturation (a), N_2-saturation (b), N_2-saturation with 320 μM H_2O_2 (c) pH 7 Tris–HCl solution, (B) plot of photocurrent intensity every 20 s after adding 10 mM glucose (irradiation wavelength = 505 nm; t_{light} = 10 s; E = −0.2 V vs. SCE) at GOx/CdTe/FTO electrode.

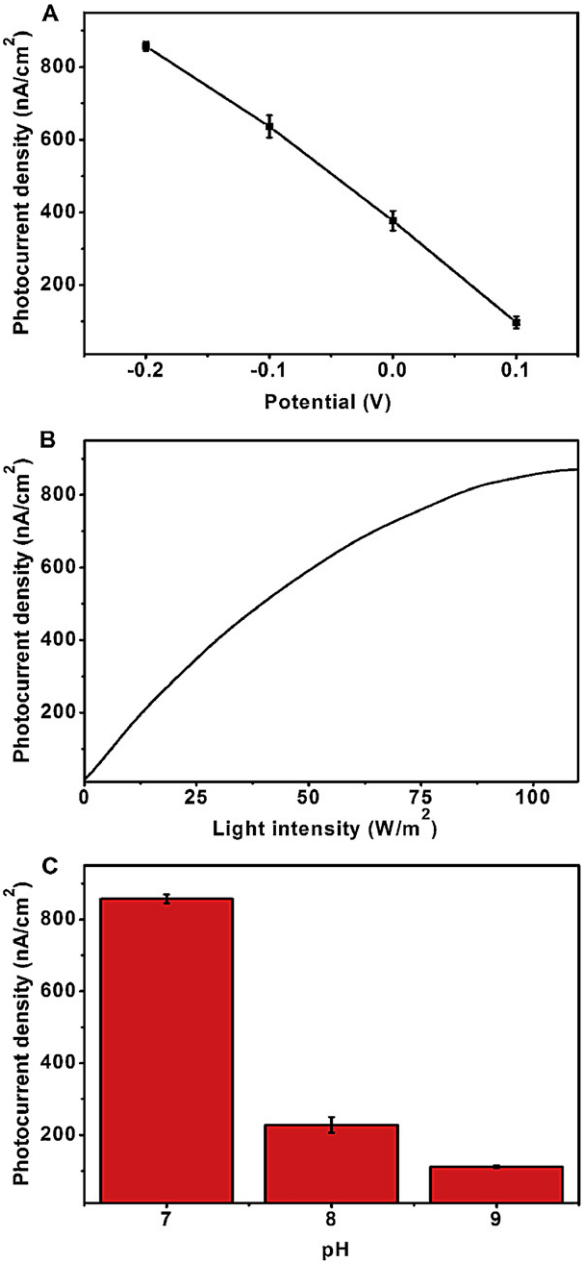

Fig. 4. Effects of (A) potential, (B) light intensity, and (C) pH of 0.1 M Tris–HCl buffer on photocurrent responses of CdTe/FTO electrode (error bar results from three independent electrodes).

3.4. Optimization of experimental conditions

The applied potential is an important factor that is relevant to the photocurrent response. On account of the elimination of interference from other reductive species that coexisted in the samples, low applied potentials ranging from −0.2 V to +0.1 V vs. SCE were investigated. Fig. 4A illustrated that the response photocurrents linearly decreased with the increasing of potential from −0.2 V to +0.1 V. Therefore, an optimal potential of −0.2 V vs. SCE was selected for the photocurrent measurements.

Irradiation light intensity is another significant factor relevant to the photocurrent response. Static photocurrent measurement was carried out from 0 to 110 W m^{-2} stepping with 2 W m^{-2}. Fig. 4B showed that the response photocurrent sharply increased at the beginning, and then reached a pseudo-plateau above 100 W.

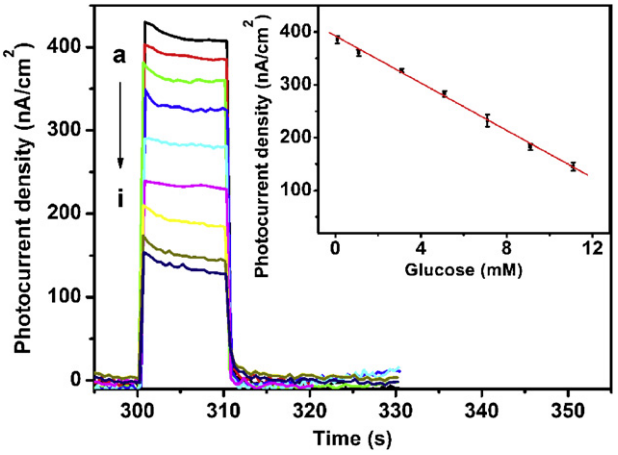

Fig. 5. Photocurrent response of a sensor in presence of (a–i) 0, 0.1, 1.1, 3.1, 5.1, 7.1, 9.1, 11.1 and 13.1 mM glucose (0.1 M pH 7.0 Tris–HCl; t_{light} = 10 s; E = −0.2 V vs. SCE). Inset: plot of photocurrent intensity vs. glucose concentration.

Considering the decreasing of the photocurrent after coating GOx, 100 W m^{-2} was chosen as the optimized light intensity.

The cathodic photocurrent intensity also depended on the pH of electrolyte. To investigate the pH influence, the photocurrent was measured in Tris–HCl with different pH. As shown in Fig. 4C, the photocurrent intensities decreased with the increasing of pH values from 7.0 to 9.0, which may be attributed to that OH^- attacked Cd^{2+} on the surface of QDs, hindering the electron transfer from QDs to O_2 when the pH becomes alkaline. Thus, pH 7.0 Tris–HCl buffer was used throughout the following experiments.

The wavelength is an important factor to the photocurrent response. At the applied potential of −0.2 V, the photocurrent decreased as the exciting wavelength increased from 485 to 535 nm. The photocurrent intensity at 505 nm was 91% of that at 485 nm, showing enough sensitivity for photoelectrochemical detection. Thus, 505 nm was chosen for the following photoelectrochemical experiments.

3.5. Detection of glucose

The oxygen sensitivity of the as-prepared QDs provides the basis for constructing the enzyme-based photoelectrochemical biosensing platform with the consumption of O_2. To verify the photoelectrochemical mechanism, using GOx as model enzyme, a convenient biosensor based on the QDs was constructed for the detection of glucose. Photocurrent measurement of GOx/CdTe/FTO electrode shows clearly signal change after adding 10 mM glucose at −0.2 V vs. SCE. As shown in Fig. 3B, the photocurrent decreases dramatically accompanying the enzymatic reaction, which is consistent with the dependence of the oxygen-sensitive photocurrent (Fig. 3A). The photocurrent reaches a pseudo-plateau after 300 s, and exhibits outstanding stability of the sensor. This phenomenon further evidenced that the photocurrent decreased upon consumption of dissolved O_2 and thus could be applied in the construction of oxidase-based photoelectrochemical biosensor.

Under optimal conditions, Fig. 5 depicts the typical time-based photocurrent response of the photoelectrochemical biosensor in the presence of different concentrations of glucose. The cathodic photocurrent is proportional to the concentration of glucose, which results from the consumption of dissolved O_2, a more efficient acceptor than the formed H_2O_2, in the enzymatic oxidation of glucose by O_2 as follows:

$$\text{glucose} + O_2 \xrightarrow{\text{GOx}} \text{gluconolactone} + H_2O_2.$$

Table 1
Determination of glucose in 5% commercial glucose injections containing glucose and sodium chloride.

Sample	Dilution	Added (mM)	Founded (mM)	Recovery (%)
1	100-fold	0	2.51 ± 0.08	96.4
		2.5	4.92 ± 0.18	
2	100-fold	0	2.48 ± 0.08	96.0
		2.5	4.88 ± 0.14	

The biosensor showed rapid response to glucose with a linear range of 0.1–11 mM at the applied potential of −0.2 V under illumination with light of 505 nm. The linear response range of the biosensor is wider than 0.2–8 mM of the voltammetric strategy using molecularly imprinted polymeric micelles [32], 0.1–2.0 mM of fluorescence resonance energy transfer between two QDs [33]. The upper detection limit of 11 mM is higher than 4.8 mM of amperometric biosensor using GOx/gold nanoparticle/ITO electrode [34] and 1.4 mM of the electrode using graphite nanosheet–Nafion composite film [35]. The detection limit of this method was estimated to be 0.04 mM at a signal-to-noise ratio of 3, which was lower than 0.7 mM of electrochemical biosensor using graphene–CdS nanocomposite [36]. Since the blood-glucose level normally maintained between 4.0 and 6.0 mM, the high upper detection limit is suitable for the practical application in blood sugar monitoring.

The photoelectrochemical biosensor for the detection of glucose showed good fabrication reproducibility with a relative standard deviation of 5.1% estimated from the slopes of the calibration plots of five freshly prepared GOx/QDs/FTO electrodes. At the glucose concentrations of 0.1 and 9 mM, the relative standard deviations examined for five determinations are 3.8% and 5.4%, respectively. These results suggest that the accuracy of the photoelectrochemical sensor is satisfactory.

After a storage time of one week in moist condition at 4 °C with measurements in pH 7.0 Tris–HCl every few days, no obvious decrease in the photocurrent response to glucose was observed. After four weeks, the photocurrent response still retained 92.3% value of the initial response, thereby suggesting acceptable stability and lifetime of the biosensor.

3.6. Application

The interference of uric acid, ascorbic acid and sodium chloride was investigated in the detection of glucose. Although both uric acid and ascorbic acid can enhance the photocurrent, sodium chloride has no effect even in 100-fold concentration in the detection of glucose. The proposed biosensor was used to determine glucose in pharmaceutical injection to indentify its feasibility. The 100-fold dilution of 5% glucose injection was found 2.5 mM of glucose. After spiking with 2.5 mM of glucose, the response current increased with a recovery of over 96.0% (Table 1). These acceptable results illustrated the photoelectrochemical biosensor was successfully applied in the analysis of real sample.

4. Conclusions

A visible light induced photoelectrochemical biosensor was developed for the detection of glucose based on oxygen-sensitive NIR QDs. The decline in aggregation and the homogeneous surface structure of the formed QD film were favorable for improving the photoelectrochemical efficiency. Due to the emission peak of the as-prepared CdTe QDs within the NIR spectral region, the resulting biosensor exhibited significant cathodic photocurrent with relatively long-wavelength light excitation, which could reduce the interference from the samples. Moreover, oxygen was indentified to be more efficient electron acceptor than the formed H_2O_2 in the enzymatic oxidation of glucose. Based on the oxygen-consuming via enzyme reaction, the designed photoelectrochemical biosensing platform shows good performances with high upper detection limit, acceptable stability and accuracy, and easy operation, providing an alternative method with good biocompatibility for monitoring biomolecules and extending the application of near-infrared QDs in bioanalysis.

Acknowledgements

We gratefully acknowledge the financial support of the National Natural Science Foundation of China (21135002, 21121091, 21075060, 20835006), the program for New Century Excellent Talents in University (NCET100479), and Science Foundation of Jiangsu (BK2010302).

References

[1] N. Haddour, J. Chauvin, C. Gondran, S. Cosnier, J. Am. Chem. Soc. 128 (2006) 9693–9698.
[2] J. Tanne, D. Schäfer, W. Khalid, W.J. Parak, F. Lisdat, Anal. Chem. 83 (2011) 7778–7785.
[3] D. Chen, H. Zhang, X. Li, J.H. Li, Anal. Chem. 82 (2010) 2253–2261.
[4] X.R. Zhang, S.G. Li, X. Jin, S.S. Zhang, Chem. Commun. 47 (2011) 4929–4931.
[5] Y.T. Long, C. Kong, D.W. Li, Y. Li, S. Chowdhury, H. Tian, Small 7 (2011) 1624–1628.
[6] G.L. Wang, J.J. Xu, H.Y. Chen, S.Z. Fu, Biosens. Bioelectron. 25 (2009) 791–796.
[7] W.W. Tu, J.P. Lei, P. Wang, H.X. Ju, Chem. Eur. J. 17 (2011) 9440–9447.
[8] A. Ikeda, M. Nakasu, S. Ogasawara, H. Nakanishi, M. Nakamura, J. Kikuchi, Org. Lett. 11 (2009) 1163–1166.
[9] M.M. Liang, S.L. Liu, M.Y. Wei, L.H. Guo, Anal. Chem. 78 (2006) 621–623.
[10] J. Chamier, J. Leaner, A.M. Crouch, Anal. Chim. Acta 661 (2010) 91–96.
[11] J.K. Jaiswal, H. Mattoussi, J.M. Mauro, S.M. Simon, Nat. Biotechnol. 21 (2003) 47–51.
[12] J.M. Klostranec, W.C.W. Chan, Adv. Mater. 18 (2006) 1953–1964.
[13] D. Ghosh, S. Ghosh, A. Saha, Anal. Chim. Acta 675 (2010) 165–169.
[14] D.R. Larson, W.R. Zipfel, R.M. Williams, S.W. Clark, M.P. Bruchez, F.W. Wise, W.W. Webb, Science 300 (2003) 1434–1436.
[15] S. Kim, Y.T. Lim, E.G. Soltesz, A.M. De Grand, J. Lee, A. Nakayama, J.A. Parker, T. Mihaljevic, R.G. Laurence, D.M. Dor, L.H. Cohn, M.G. Bawendi, J.V. Frangioni, Nat. Biotechnol. 22 (2004) 93–97.
[16] G.X. Liang, H.C. Pan, Y. Li, L.P. Jiang, J.R. Zhang, J.J. Zhu, Biosens. Bioelectron. 24 (2009) 3693–3697.
[17] Z. Qian, H.J. Bai, G.L. Wang, J.J. Xu, H.Y. Chen, Biosens. Bioelectron. 25 (2010) 2045–2050.
[18] D.R. Cooper, N.M. Dimitrijevic, J.L. Nadeau, Nanoscale 2 (2010) 114–121.
[19] A.L. Rogach, A. Eychmüller, S.G. Hickey, S.V. Kershaw, Small 3 (2007) 536–557.
[20] Q. Ma, X.G. Su, Analyst 135 (2010) 1867–1877.
[21] G.X. Liang, H.Y. Liu, J.R. Zhang, J.J. Zhu, Talanta 80 (2010) 2172–2176.
[22] Q. Kang, L.X. Yang, Y.F. Chen, S.L. Luo, L.F. Wen, Q.Y. Cai, S.Z. Yao, Anal. Chem. 82 (2010) 9749–9754.
[23] Z.G. Xiong, X.S. Zhao, J. Am. Chem. Soc. 134 (2012) 5754–5757.
[24] M.Y. Gao, S. Kirstein, H. Möhwald, A.L. Rogach, A. Kornowski, A. Eychmüller, H. Weller, J. Phys. Chem. B 102 (1998) 8360–8363.
[25] J.S.W. Mak, A.A. Farah, F.F. Chen, A.S. Helmy, ACS Nano 5 (2011) 3823–3830.
[26] W.W. Yu, L.H. Qu, W.Z. Guo, X.G. Peng, Chem. Mater. 15 (2003) 2854–2860.
[27] H. Borchert, D.V. Talapin, N. Gaponik, C. McGinley, S. Adam, A. Lobo, T. Möller, H. Weller, J. Phys. Chem. B 107 (2003) 9662–9668.
[28] N.A. Shah, A. Ali, S. Hussain, A. Maqsood, J. Coat. Technol. Res. 7 (2010) 105–110.
[29] H. Nakanishi, K.J.M. Bishop, B. Kowalczyk, A. Nitzan, E.A. Weiss, K.V. Tretiakov, M.M. Apodaca, R. Klajn, J.F. Stoddart, B.A. Grzybowski, Nature 460 (2009) 371–375.
[30] L.H. Tang, Y.H. Zhu, X.L. Yang, J.J. Sun, C.Z. Li, Biosens. Bioelectron. 24 (2008) 319–323.
[31] D.R. Lide, CRC Handbook of Chemistry and Physics, 88th ed., CRC Press Inc., Boca Raton, 2008.
[32] Y.Q. Yang, C.L. Yi, J. Luo, R. Liu, J.K. Liu, J.Q. Jiang, X.Y. Liu, Biosens. Bioelectron. 26 (2011) 2607–2612.
[33] B. Hu, L.P. Zhang, M.L. Chen, M.L. Chen, J.H. Wang, Biosens. Bioelectron. 32 (2012) 82–88.
[34] J.W. Wang, L.P. Wang, J.W. Di, Y.F. Tu, Sens. Actuators B 135 (2008) 283–288.
[35] C.L. Fu, W.S. Yang, X. Chen, D.G. Evans, Electrochem. Commun. 11 (2009) 997–1000.
[36] K. Wang, Q. Liu, Q.M. Guan, J. Wu, H.N. Li, J.J. Yan, Biosens. Bioelectron. 26 (2011) 2252–2257.